Sensors and Actuators B 262 (2018) 958–965

Contents lists available at ScienceDirect

Sensors and Actuators B: Chemical

journal homepage: www.elsevier.com/locate/snb

A FRET chemosensor for hypochlorite with large Stokes shifts and long-lifetime emissions

Zhiwei Liu [a], Fengling Song [a,*], Bo Song [b], Long Jiao [a], Jing An [a], Jingli Yuan [b], Xiaojun Peng [a]

[a] State Key Laboratory of Fine Chemicals, Dalian University of Technology, Dalian 116024, PR China
[b] School of Chemistry, Dalian University of Technology, Dalian 116024, PR China

ARTICLE INFO

Article history:
Received 4 December 2017
Accepted 30 January 2018
Available online 2 February 2018

Keywords:
FRET
Chemosensor
Hypochlorite
Long-lifetime
Time-resolved imaging

ABSTRACT

A FRET-based chemosensor for hypochlorite was developed, both the donor and acceptor of this FRET system are fluorophores with a large Stokes shift. The donor has two comparable excitation peaks at 460 nm and 575 nm. And it is found FRET-sensitized emission has less interference from direct-excited acceptor emission when excitation at 460 nm compared with excitation at 575 nm. The sensitivity can be improved for 4-fold (<95 nM). Meanwhile the donor can be excited by two-photon excitation source, which is an anti-Stokes shift property. It makes the chemosensor totally to get rid of the direct-excited acceptor emission for the FRET sensing method. Furthermore, the long lifetime luminescence of the FRET pairs makes them possible to be used in time-resolved technology, this can overcome the autofluorescence interference from biological matrix. All above characters implied this FRET pairs have more potential to be applied in hypochlorite detection of biological samples.

1. Introduction

During the last 40 years, Förster or fluorescence resonance energy transfer (FRET) measurement method has been widely used for the detection and quantification of biochemical activities [1]. Many ratiometric fluorescence probes or chemosensors based on FRET have been developed in biology analysis field [2,3]. The ratiometric measurement of acceptor to donor fluorescence of the FRET pairs provide a built-in correction for environmental effects [4]. However, the accurate ratiometric quantification of FRET is affected by the choice of donor-acceptor fluorophore pairs [5,6]. A very common deviation comes from the spectral cross-talks, including donor spectral bleed-through (donor emission into acceptor channel) and direct-excited acceptor emission (direct excitation of acceptor fluorophores by donor excitation) [7]. Although efforts including optimization of pairings and detection conditions for measurement of FRET were carried out, uncorrected ratiometric signals are not yet reliable [8,9]. Many complicate linear unmixing algorithms have been used to achieve more accurate FRET efficiency quantitatively by correction tools [10,11]. Howbeit, the ultimate reason for deviation is that almost all chromophores for FRET pairs have a small Stokes shift which causes the overlap of fluorophore spectra. It is very desirable to develop new FRET pairs with large Stokes shift, which can assure more accurate FRET measurement without corrections.

In our previous work, we reported an example for FRET spectra unmixing [12]. A ratiometric fluorescent nanoprobe for hypochlorite was developed with a big spectral separation (175 nm) between the donor (Rhodamine B) emission and the acceptor (an aminocyanine dye Cy7-N) emission. This resolves the problem of donor emission bleed-through into acceptor channel. But the FRET-sensitized emission and direct-excited acceptor emission cannot be resolved because of the direct excitation of acceptor fluorophores by donor excitation at 550 nm.

Time-resolved FRET (TR-FRET) technology is an emerging alterative tool aiming for more accurate FRET measurement without complicate spectral unmixing algorithms [13]. The two key characters of lanthanides: large Stokes shift and long-lived luminescence, make them the best candidates for the donors of TR-FRET [14]. Since the Stokes shifts of lanthanide chelates or nanocrystals are usually more than 200 nm, direct-excited acceptor emission can be avoided when using lanthanides as FRET donors. And the luminescence lifetime of lanthanides is up to milliseconds make them suitable for TR-FRET detection to completely suppress the interference of short-lived auto-fluorescence from the background which is less than 10 nanoseconds [15]. However, the cytotoxicity of these heavy metal-based complexes is still a big concern for practical application. And the size of lanthanide nanocrystals is usually around 20 nm, which

* Corresponding author.
E-mail address: songfl@dlut.edu.cn (F. Song).

https://doi.org/10.1016/j.snb.2018.01.240
0925-4005/

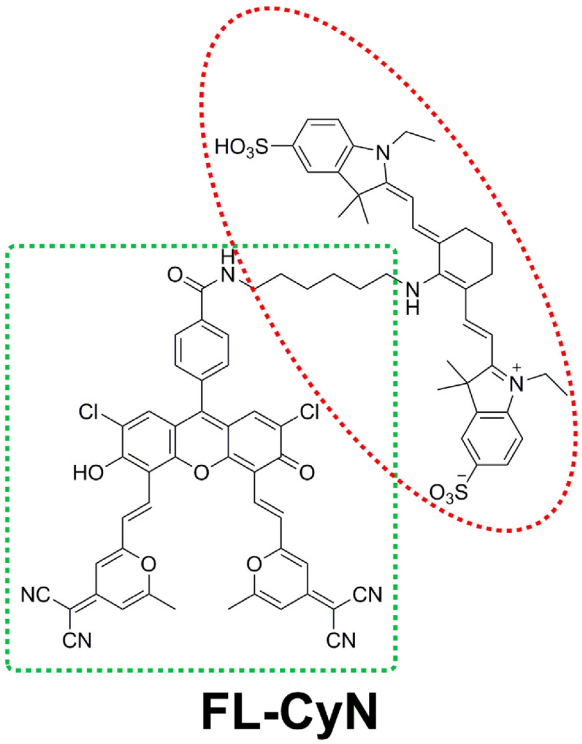

Scheme 1. The molecular structure of the chemosensor **FL-CyN**, the green square part is the donor **FL**, the red oval part is the acceptor **CyN**. (For interpretation of the references to colour in this scheme legend, the reader is referred to the web version of this article.)

is not appropriate when considering the FRET distance radius is in the range of 2–10 nm [16]. So, it is very desirable to develop new FRET donor with large Stokes shift, small size and low toxicity. If the donor has long luminescence lifetime, it will be able to be used in TR-FRET in lieu of lanthanides.

Here we develop such a new FRET-based chemosensor **FL-CyN** for hypochlorite (Scheme 1). Both donor and acceptor have a large Stokes shift. The acceptor is an aminocyanine dye **CyN** which is developed in our group in 2005 [17]. Besides having a large Stokes shift, **CyN** is also used as an oxidative stress sensing part [18–20]. And the donor is a new fluorescein derivative **FL** which was recently found by our research group to have a large Stokes shift and a long-lifetime luminescence [21]. This new donor provides the chemosensor **FL-CyN** not only a big spectral separations of FRET pairs' emissions, but also the distinction of the FRET-sensitized and direct-excited acceptor emission due to the donor's large Stokes shift. Moreover, the potential long-lifetime luminescence and two-photon excitation properties of the donor make the chemosensor work in TR-FRET measurement and in near-infrared spectrum region, which benefit the bioanalysis more accurate and desirable. Importantly, both donor and acceptor are organic fluorophores whose toxicity is believed very low. Because their mother molecules (Fluorescein and Indocyanine Green) are only the two fluorophores which are currently approved by the U.S. Food and Drug Administration (FDA) for medical use [22].

2. Experimental section

2.1. Reagents

All the reactions were carried out under a nitrogen atmosphere with dry, freshly distilled solvents under anhydrous conditions, unless otherwise noted. Silica gel (100–200 mesh) was used for flash column chromatography. Ultrapure deionized water from a Milli-Q ultrapure system was used for all synthesis, dialysis, and storage steps.

2.2. Apparatus

^{1}H NMR and ^{13}C NMR spectra were recorded on a VARIAN INOVA-400 spectrometer with chemical shifts reported as ppm (TMS as internal standard). Mass spectrometric data were obtained on Q-TOF Micro mass spectrometry and LTQ Orbitrap XL mass spectrometry. Fluorescence spectroscopy were recorded on a fluorometer (Cary Eclipse from Agilent Tech). The data were obtained under the control of a Windows-based PC running the manufacturers' supplied software. The confocal microscopy imaging was used OLYMPUS FV-1000 inverted fluorescence microscope. The absorbance for MTT analysis was recorded on a microplate reader (Thermo).

2.3. Synthesis of the FL-CyN

The synthesis of **FL-CyN** was carried out by using a classic coupling reaction between the amino group in **CyN** and the carboxyl group in **FL** (Schemes S1–3). The 1H NMR and 13C NMR spectra of **FL-CyN** are given in supporting information (ESI).

2.4. FRET efficiency analysis

Experimentally, FRET efficiency E calculated from donor was determined using

$$E(D) = \frac{F_D - F_{DA}}{F_D}$$

where F_D and F_{DA} designate the integrated fluorescence intensities of donor alone and donor in the presence of acceptor, respectively.

However, FRET efficiency E calculated from acceptor was determined using

$$E(A) = \frac{F_{DA} - F_A}{F_{DA}}$$

where F_A and F_{DA} designate the integrated fluorescence intensities of acceptor alone and donor in the presence of acceptor, respectively.

2.5. Zebrafish and culture conditions

Zebrafish was purchased from the Nanjing Eze-rinka Biotechnology company (Nanjing, China). Zebrafish were cultured in medium and incubated at 28 °C in air.

2.6. Confocal microscopy imaging of zebrafish

The zebrafish was incubated in a glass bottom dish (NEST, 35 mm dish with a 20 mm bottom well) with **FL-CyN** for 2 h at 28 °C. Before the confocal laser scanning microscopy observation, the zebrafish were washed 3 times with probe-free medium to fully remove the uninternalized probe. Fluorescence imaging was performed using an OLYMPUS FV-1000 inverted fluorescence microscope with a 4× objective lens. Then the same sample was treated with exogenous HClO for 20 min, Before the confocal laser scanning microscopy observation, the zebrafish were washed 3 times with HClO-free medium to fully remove the exogenous HClO. Fluorescence images was collected at 575–620 nm (green channel) and 655–755 nm (red channel) upon excitation at 488 nm and 559 nm.

2.7. The test of two-photon absorption cross-section

The test of two-photon absorption (TPA) cross-section were measured from Z-Scan measurement, the minima characterize the TPA of the sample in the beam focus. A Gaussian fit was used to analyze the data and to determine the transmission T at the minimum. The TPA cross section σ was calculate using

$$\sigma = \frac{(1-T)E_P}{TlI_0N_Ac^2}$$

where Ep is the photo energy, l is the sample path length, I_0 is the input power, NA is the Avogadro constant, and c is the sample concentration.

2.8. Two-photon confocal luminescence images of zebrafish

The zebrafish was incubated in a glass bottom dish (NEST, 35 mm dish with a 20 mm bottom well) with 10 μM probe at 28 °C for 2 h, then the zebrafish was washed 3 times with probe-free medium to fully remove the uninternalized probe, fluorescence imaging was performed using an OLYMPUS FV-1000 inverted fluorescence microscope with a 4× objective lens. Then the same sample was incubation with 100 μM HClO for 20 min. Before the confocal laser scanning microscopy observation, the zebrafish were washed 3 times with medium to fully remove the exogenous HClO. Fluorescence imaging was performed using an OLYMPUS FV-1000 inverted fluorescence microscope with a 4× objective lens. Fluorescence images was collected at 575–620 nm upon two-photon excitation at 800 nm.

2.9. Time-resolved luminescence images of zebrafish

The zebrafish was incubated in a glass bottom dish (NEST, 35 mm dish with a 20 mm bottom well) with 10 μM probe and 4 μM BSA at 28 °C for 2 h, then the zebrafish was washed 3 times with probe-free medium to fully remove the uninternalized probe, fluorescence imaging was performed using a time-resolved fluorescence microscope with a 4× objective lens. Then the same sample was incubation with 100 μM HClO for 20 min. Before the confocal laser scanning microscopy observation, the zebrafish were washed 3 times with medium to fully remove the exogenous HClO. Fluorescence imaging was performed using a time-resolved fluorescence microscope with a 4× objective lens. Fluorescence images was collected at 590–650 nm upon excitation at 450 nm.

2.10. Cell and culture conditions

MCF-7 cell line was purchased from the Chenyu biological company (Dalian, China). MCF-7 cells were cultured in Dulbecco's modified Eagle medium (DMEM; GIBCO) containing 10% fetal bovine serum (FBS; GIBCO). Cultured cells were incubated at 37 °C in an atmosphere of 5% CO_2 in incubator.

2.11. MTT assay

MCF-7 cells were used to evaluate the cytotoxicity of **FL-CyN** using the methyl terazolium (MTT). The cells were seeded at a density of 1×10^5 cells/mL in a 96-well plate for 24 h at 5% CO_2 atmosphere, then incubated with **FL-CyN**, **FL**, **CyN**, Fluorescein and ICG at different concentration of 5 μM, 10 μM, 15 μM, 20 μM for 8 h, then MTT tetrazolium solution was added to each well incubated at 37 °C for another 4 h. The MTT tetrazolium solution was removed from the wells carefully, and the colored formazan was dissolved in 150 μL of dimethyl sulfoxide (DMSO). The plate was shaken for 3 min and the absorbance of the solutions in the wells was measured at 490 nm using a Multiskan FC-microplate reader.

3. Results and discussion

3.1. FRET mechanism of the chemosensor FL-CyN

The absorption of **FL-CyN** contains a peak at 460 nm and a peak at 630 nm which belong to the donor and the acceptor respectively (Fig. S1). From Fig. 1a, a good overlap between the emission of **FL** and the absorption of **CyN** assure the occurrence of FRET in the chemosensor **FL-CyN**. And in the emission spectra of **FL-CyN**, strong emission peak at 750 nm assigning to the acceptor can be seen while weak emission peak of the donor at 630 nm can be found (Fig. 1b). This result indicates that an efficient intramolecular FRET does occur. Meanwhile, the intermolecular FRET cannot happen for the same donor and acceptor system (Fig. S2a) by simply mixing the two compounds of **FL** and **CyN**.

The first thing we try to explore how the large Stokes shift of the donor will affect the FRET measurement. As shown in Fig. 2a, the donor **FL** has almost the same fluorescence intensity when excited at 575 nm or 460 nm. This means that **FL** will have the same energy transfer capability when used as the FRET donor by excited either at 575 nm or 460 nm. The excitation spectrum tells the same story as shown from Fig. 2b. However, when **FL-CyN** was excited at 575 nm or 460 nm respectively, the obtained fluorescence spectra have the different fluorescence intensity in the acceptor's emission region. The intensity achieved by excitation at 575 nm is much stronger than that by excitation at 460 nm (Fig. 2c). From Fig. 2d, we knew the acceptor alone can be obviously excited by 575 nm but almost not by 460 nm. It is reasonable to conclude that direct-excited acceptor emission when excited by 575 nm will interfere the FRET-sensitized emission, which is a common phenomenon for almost all FRET donor-acceptor pairs with a small Stokes shift. But, in our case the fluorescence intensity obtained by excitation at 460 nm can more accurately representatives the FRET-sensitized energy transfer. This result can also be demonstrated by the data of FRET efficiency. As shown in case A in Table 1, there is no big difference for the calculated FRET efficiency based on the emission intensity of the donor when the FRET data were obtained by excitation at 460 nm or 575 nm. The big or small Stokes shift of the donor

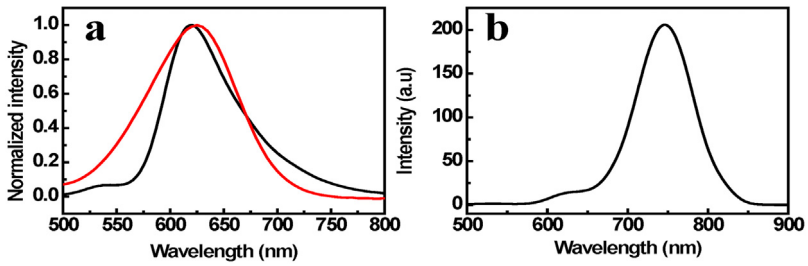

Fig. 1. (a) The UV-spectra of **CyN** (black line) in PBS/CH_3CH_2OH (1:2 v/v) and the fluorescence spectra of **FL** (red line) in PBS/CH_3CH_2OH (1:2 v/v) at excitation wavelength of 460 nm. (b) The fluorescence spectra of **FL-CyN** in PBS/CH_3CH_2OH (1:2 v/v) with excitation at 460 nm. (For interpretation of the references to colour in this figure legend, the reader is referred to the web version of this article.)

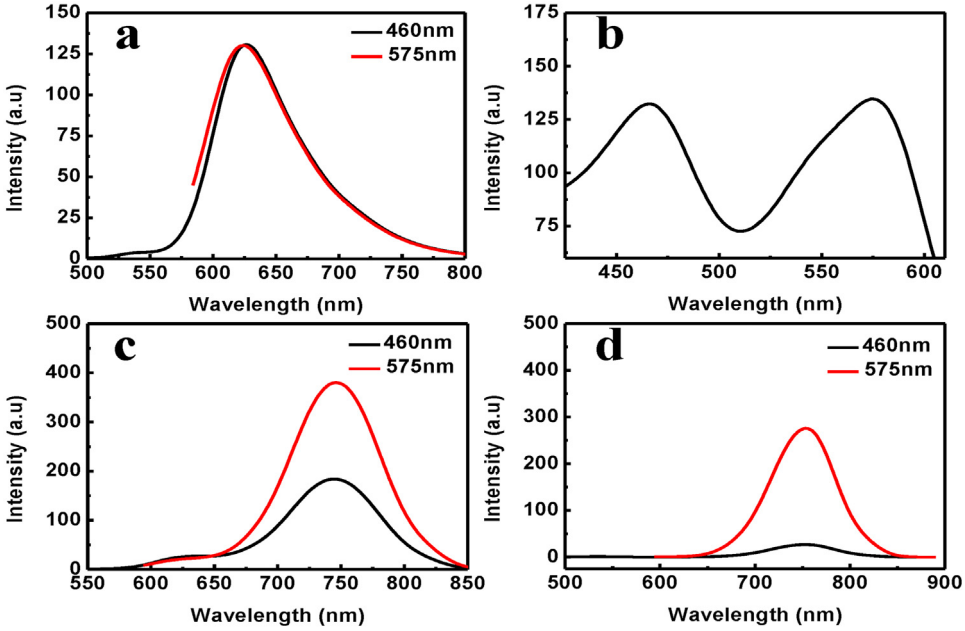

Fig. 2. (a) The fluorescence spectra of **FL** (5 μM) in PBS/CH_3CH_2OH (1:2 v/v) at excitation wavelength of 460 nm and 575 nm; (b) The excitation spectra of **FL** (5 μM) in PBS/CH_3CH_2OH (1:2 v/v), λex = 630 nm; (c) The fluorescence spectra of **FL-CyN** (5 μM) in PBS/CH_3CH_2OH (1:2 v/v) at excitation wavelength of 460 nm and 575 nm; (d) The fluorescence spectra of **CyN** (5 μM) in PBS/CH_3CH_2OH (1:2 v/v) at 460 nm and 575 nm.

Table 1
The FRET efficiency was calculated based on the emission intensity change of the donor or that of the acceptor. There is a big difference between the efficiency obtained by excited at 460 nm and 575 nm.

case	FRET efficiency	λem = 460 nm	λem = 575 nm
A	based on donor	90%	88%
B	based on acceptor	88%	40%

Table 2
Fluorescence lifetime compositions of delayed components of **FL-CyN** (5 μM) with BSA (4 μM) in room temperature under atmosphere, Excited at 465 nm (Spectral LED-460) and monitored at 630 nm and 754 nm.

	τ_1(μs)[a]	n_1%[b]	τ_2(μs)[a]	n_2%[b]	τ_3(μs)[a]	n_3%[b]	τ_d(μs)[c]
630 nm	108	0.04	29.8	0.50	9.76	0.47	23.8
754 nm	9.51	0.40	28.5	0.21	0.28	0.39	9.90

[a] Obtained from the double-exponential fitting of transient decay curves on a 680 μs scale.
[b] The contribution of each component to average lifetime.
[c] The average fluorescence lifetime of delayed component.

does not affect the calculated FRET efficiency. This explains why the FRET efficiency is preferentially calculated based on the emission intensity change of the donor in the presence of the acceptor or without the presence of the acceptor. But, as shown in the case B of Table 1, there is a big difference for the calculated FRET efficiency based on the emission of the acceptor. When excited at 575 nm, the FRET efficiency is 40% which is obviously deviate from the truth. This means direct-excited acceptor emission is about fifty percent proportion of total acceptor's emission intensity when excitation at 575 nm, which is consistent with the data shown in Fig. 2c and d. And the FRET efficiency is 88% when excitation at 460 nm. That means direct-excited acceptor emission is almost excluded from FRET-sensitized emission when excitation at 460 nm. So, the big Stokes shift of the donor offers the current donor-acceptor pairs a more real FRET determination.

3.2. The long lifetime of FL-CyN

The more accurate FRET determination can be strengthened by another advantage offered by the donor **FL**. This donor was found to have a thermally activated delayed fluorescence in our previous study [21], which provides the FRET system long-lifetime luminescence for both donor and acceptor (τ = 23.8 μs and 9.90 μs, see Table 2 and Fig. 3). This character can be used in time-resolved FRET imaging technologies to diminish the false positive signal from autofluorescence of biological matrix in both donor and acceptor's signal window, because the lifetime of biological autofluorescence is usually in nanosecond level [23]. Moreover, this character offers the this FRET pairs can be used in fluorescence lifetime FRET imaging technique (FRET-FLIM) which is considered as a powerful tool for quantitative measurement with more higher accuracy [24].

3.3. The effect for sensing hypochlorite

Hypochlorite is one kind of reactive oxygen species and plays an important role of microbicidal activity. However, excess production of HOCl within phagocytes is known to be closely related to onset of a variety of human diseases [25]. A number of fluorescence probes have been reported to monitor hypochlorite [26]. The development of FRET-based fluorescence probes is one of the most promising accurate and reliable analytical methods for sensing biological HOCl in living systems [27].

As shown in Fig. S2, the FRET chemosensor **FL-CyN** can efficiently respond to hypochlorite, but no obvious change for the mixture of **FL** and **CyN** can be observed when treated with the same amount of hypochlorite. The ratiometric changing between the emissions of the donor and acceptor is well dependent with the adding amount of hypochlorite as shown in Fig. 4a.

The sensing sensitivity is one of the most important parameters for a success chemosensor. Whether the sensitivity of the FRET chemosensor can be improved by excitation at 460 nm other than at 575 nm? We checked two linear relationships between the ratio I_{631}/I_{754} and the concentration of hypochlorite by excitation at 460 nm and 575 nm, respectively, as shown in Fig. 4b. The slope based on 460 nm excitation is 4-fold larger than that based on 575 nm excitation. This result brings out that the detection limit

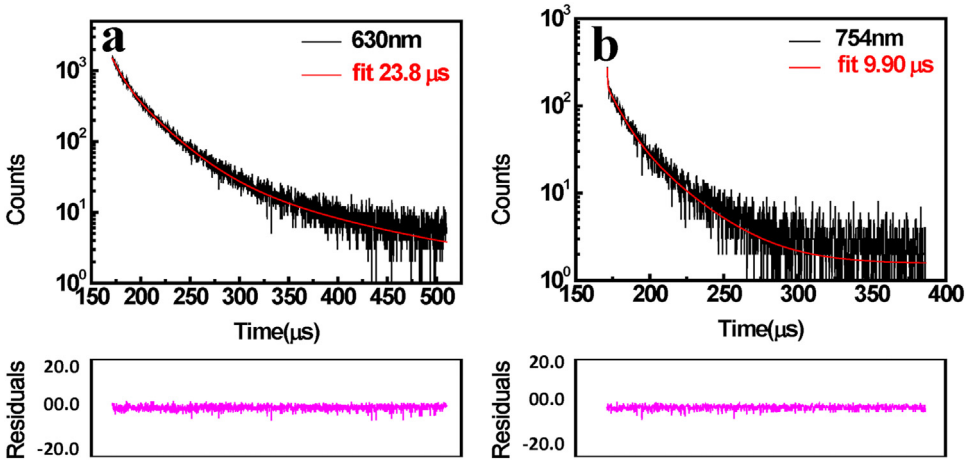

Fig. 3. Emission decays of FL-CyN (5 μM) with 4 μM BSA in PBS at room temperature, (a) Excited at 460 nm and monitored at 630 nm (τ = 23.8 μs) under atmosphere, (b) Excited at 460 nm and monitored at 754 nm (τ = 9.90 μs) under atmosphere.

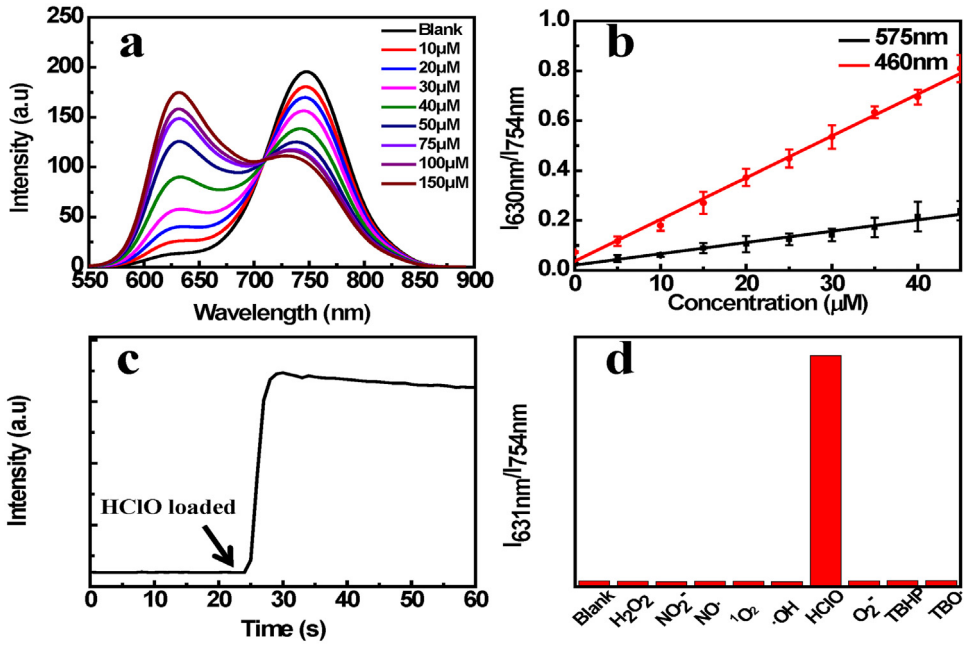

Fig. 4. (a) Fluorescence spectra of **FL-CyN** (5 μM) to HClO (0–30 equiv) in PBS/CH_3CH_2OH (1:2 v/v) at excitation wavelength of 460 nm. (b) The I631/I754 ratio response of the **FL-CyN** to different concentrations of HClO. (c) Time course of luminescence intensity of the **FL-CyN** at 631 nm upon addition HClO (200 μM). (d) The I_{631}/I_{754} ratio response of the **FL-CyN** (5 μM) toward HClO, other ROS and RNS (all in 100 μM).

with 460 nm excitation (0.095 μM) is 4-fold lower than that with 575 nm excitation (0.33 μM), which proves the large Stokes shift of the donor can improving the sensitivity of the FRET chemosensor. From Fig. 4c, the response time to HClO was found to be 5 s, much faster than our previous nanoprobe [8]. This result indicates that the **FL-CyN** can quickly respond to HClO. As shown in Fig. 4d, the ratiometric luminescence response was highly specific toward HClO over other ROS and RNS including H_2O_2, NO_2^-, $NO^{\bullet}$, $^1O_2$, $^{\bullet}OH$, O_2^-, TBHP, $TBO^{\bullet}$. A 27-fold contrast can be achieved for HClO over other ROS and RNS. All of the above results demonstrate that the **FL-CyN** is promising as a sensitive, fast and selective chemosensor for detection of HClO.

And the FRET sensing system is robust. The bleaching effect of hypochlorite can be seen only in **CyN** (Fig. S3). And **FL** is stable under oxidative stress of hypochlorite up to 500 μM (Fig. S4). The absorption changing trend of **FL-CyN** tells the same story that only the peak at 630 nm diminishes but the peak of the donor at 460 nm is kept during the oxidative bleaching process (Fig. S5). Mass spectra was used to explore the product oxidized by HOCl (Fig. S6). An epoxide product can be formed by oxidation of double bonds in the methine chain of **CyN** moiety, which is consistent with the proposed oxidation mechanism [19]. From the result of theoretical calculation (Fig. S7), the electron density of **FL-CyN** is located on the methine chain of **CyN**, which proves the sensing mechanism of acceptor oxidation. The distance between acceptor and donor is 8.91 Å (Fig. S7), which allows efficient fluorescence resonance energy transfer process between acceptor and donor of **FL-CyN**.

3.4. The sensing performance in the biological samples

Considering that **FL-CyN** has good water-solubility and is not permeable for living cells, zebrafishes were chosen as an animal model for studying the ratiometric fluorescence bioimaging. As shown in Fig. 5a, the zebrafish exhibited bright fluorescence in the red channel (acceptor emission) and dark fluorescence in the green channel (donor emission) after stained with **FL-CyN** when excita-

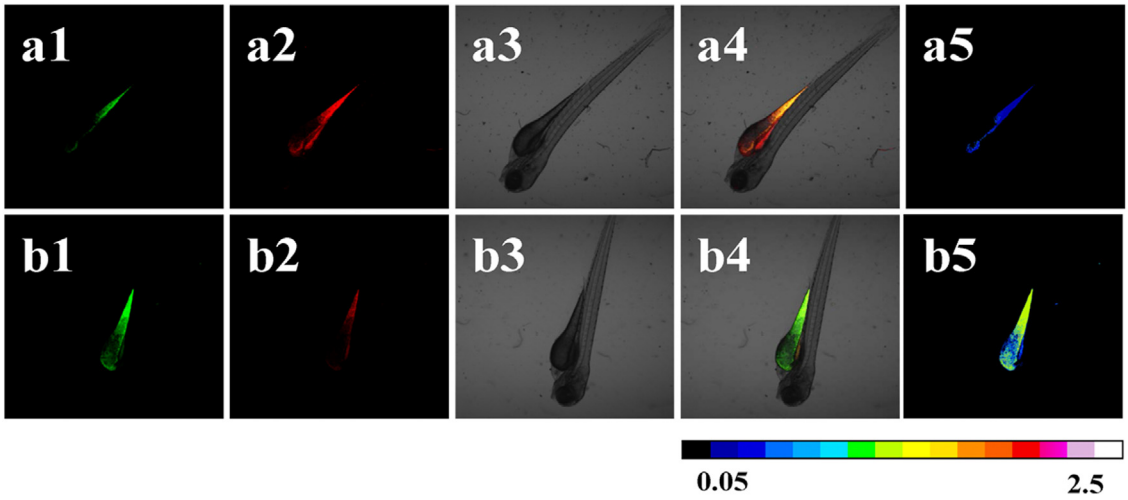

Fig. 5. Confocal luminescence (excitation at 488 nm) images of the 5-day-old zebrafish stained with **FL-CyN** (10 μM) for 1.5 h before (a1–a5) and after (b1–b5) incubation with HClO (100 μM) for 20 min. The images of a1 and b1 are fluorescence images collected at 575–620 nm. The images of a2 and b2 are fluorescence images collected at 655–755 nm. The images of a3 and b3 are the bright field images. The images of a4 and b4 are the overlap of and fluorescence images and bright field images. The images of a5 and b5 are ratiometric images of Igreen/Ired.

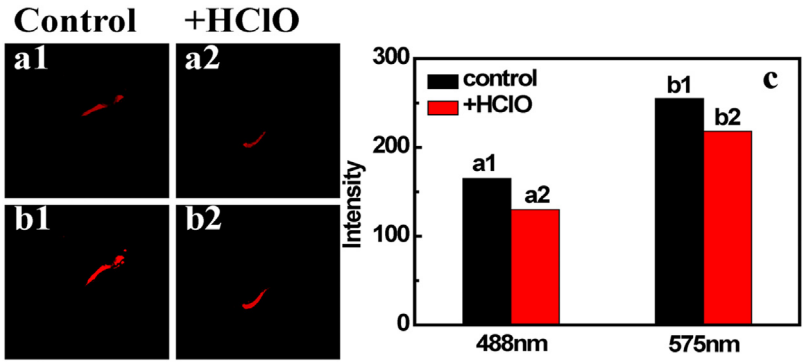

Fig. 6. Confocal luminescence images of the 5-day-old zebrafish stained with **FL-CyN** (5 μM) for 2 h by excitation at 488 nm (a1) or at 559 nm (b1). Fluorescence images are collected again after incubation with HClO (30 μM) for 20 min when excitation at 488 nm (a2) or at 559 nm (b2). The imaging window is at 655–755 nm. The corresponding fluorescence intensity of confocal luminescence images (a1 and a2 for 488 nm excitation, b1 and b2 for 559 nm excitation) were recorded in the graph (c).

tion at 488 nm. Then the same sample was treated with exogenous HClO for 20 min. A clear change was observed as shown in Fig. 5b. The fluorescence signals of the red channel obviously decreased but increased in the green channel. Quantitative analysis of the ratiometric images of these two channels shows that a more than 10-fold of the ratio value has increased after the HClO treatment from Fig. 5a5–b5.

Whether the sensitivity of the ratiometric images are also be affected for the in vivo experiments by the large Stokes shifte of the donor? We compared two available lasers at 488 nm and 559 nm of our confocal fluorescence imaging system as excitation source. As shown in Fig. S8, the ratio value obtained by excitation at 488 nm (Fig. S8-c5) is much bigger than that of excitation at 559 nm (Fig. S8-d5) when the chemosensor was treated with the same amount of hypochlorite (30 μM). This result means the excitation at 488 nm can bring out more sensitive measurement than that of excitation at 559 nm, which is consistent with the result of in vitro shown in Fig. 3b.

Besides the sensitivity are improved by excitation at 488 nm due to the large Stokes shift of the donor, the FRET-sensitized emission can be resolved from direct-excited acceptor emission for the in vivo experiment. As shown in Fig. 6, the fluorescence intensity of a1 and a2 obtained by excitation at 488 nm are much lower that of b1 and b2 obtained by excitation at 559 nm. This is because that the fluorescence intensity with 559 nm excitation contains both the direct-excited acceptor emission and the FRET-sensitized emission.

3.5. The two-photon bioimaging

The interference of direct-excited acceptor emission can be totally removed if the donor has an anti-Stokes shift. Fortunately, this special donor was found to have a two-photon excitation property. This property can totally get rid of the direct-excited acceptor emission for the FRET sensing method and achieve the more accurate FRET results. As shown in Fig. S9, both **FL** and **FL-CyN** have two-photon performance with a good two-photon absorption cross-section in the range of 780–830 nm. From Fig. 7. A clear fluorescence image for zebrafish can be collected in the window of 575–630 nm by two-photon excitation at 800 nm. Due to the lack of ratiometric imaging setting of the two-photon imager, no images were obtained at the red channel of 655–750 nm. It is worthy to note that two-photon excitation make this chemosensor promising for deep tissue imaging.

3.6. The time-resolved bioimaging

Different from conventional FRET donors which are singlet state emitters, the new donor **FL** is a triplet emitter and has a long

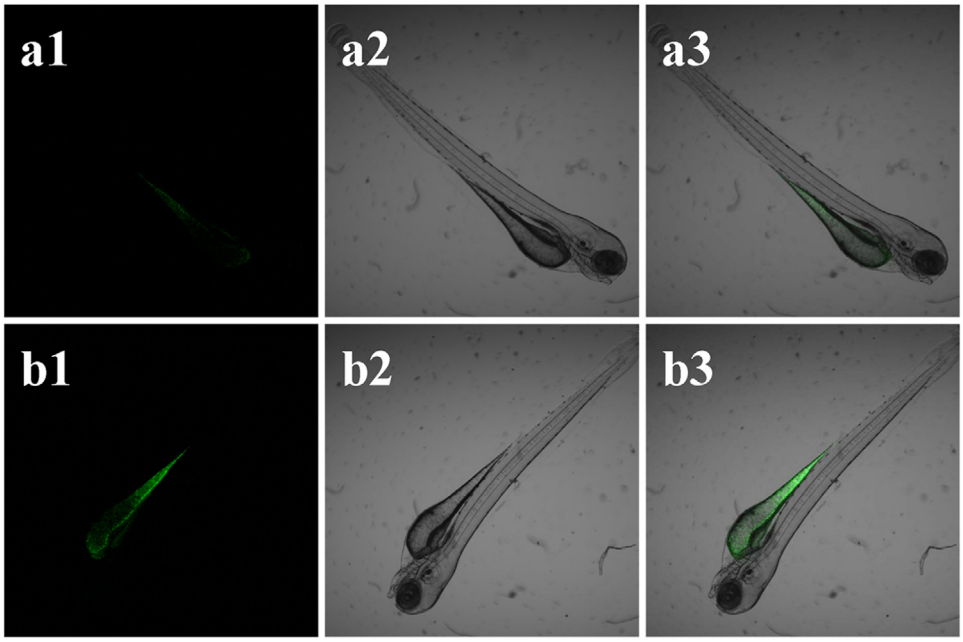

Fig. 7. Two-photon confocal luminescence (excitation at 800 nm) images of the 5-day-old zebrafish loaded with **FL-CyN** (10 μM) for 2 h before (a1–a3) and after (b1–b3) incubation with HClO (100 μM) for 20 min. The images of a1 and b1 are fluorescence images collected at 575–630 nm. The images of a2 and b2 are the bright field images. The images of a3 and b3 are the overlap of and fluorescence images and bright field images.

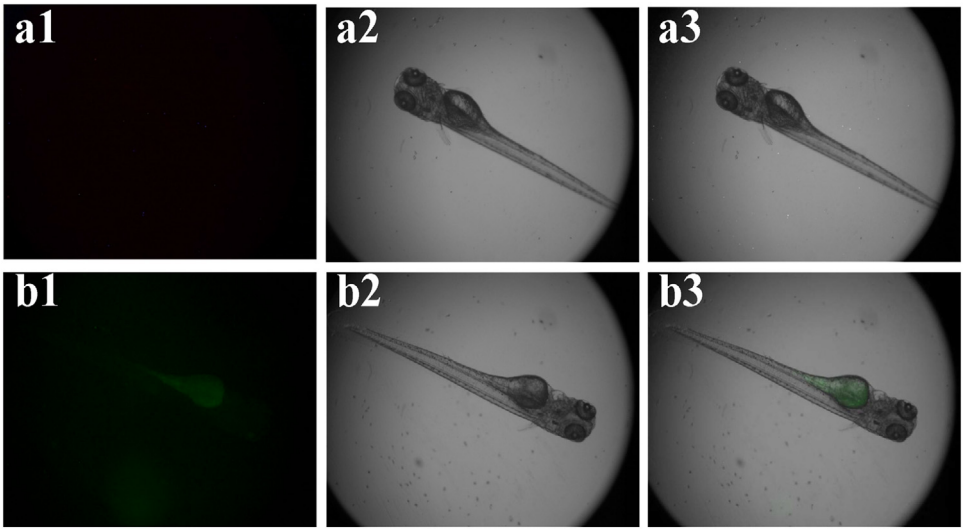

Fig. 8. Time-resolved luminescence (excited with 450 nm) images of the 5-day-old zebrafish stained with **FL-CyN** (10 μM) with 4 μM BSA for 2 h before (a1–a3) and after (b1–b3) incubation with HClO (100 μM) for 20 min. The images of a1 and b1 are time-resolved luminescence images collected at 590–650 nm. The images of a2 and b2 are the bright field images. The images of a3 and b3 are the overlap of and fluorescence images and bright field images.

life-time emission, which enables **FL-CyN** to be applied for time-resolved luminescence imaging [21]. As shown in Fig. 8b3, weak time-resolved luminescence in the abdomen of zebrafish can be collected in the window of 590–650 nm after treated with BSA (4 μM) and HClO (100 μM). The hydrophobic environment of BSA and protein inside of the zebrafishes makes both donor and acceptor emit long-lifetime emissions without removal of oxygen from the detection samples (see Fig. S10). The time-resolved ratiometric images of I_{green}/I_{red} cannot be achieved due to the lack of the red channel of 655–750 nm for the instrumental limitation. Even though, the employ of time-resolved techniques can well overcome the autofluorescence of biomatrix, which provides **FL-CyN** a big advantage for bioapplications.

3.7. The cytotoxicities

The cytotoxicities of the donor, the acceptor and the chemosensor were evaluated by MTT experiments. From Fig. 9, the cytotoxicites of **FL-CyN** and its components **FL** and **CyN** are all found to be as low toxic as the two FDA proved dyes: **ICG** and Fluorescein.

4. Conclusion

In summary, we designed a novel FRET system by using two fluorophores both with a large Stokes shift as donor-acceptor pairs. A more accurate FRET determination was achieved due to their particular characters of the two fluorophores. The special donor **FL**

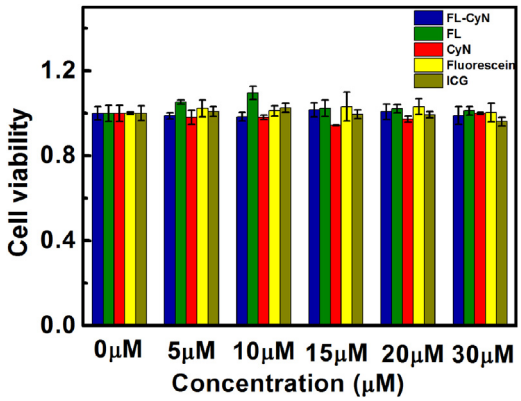

Fig. 9. In vitro cell viablity of MCF-7 cells. The cells were incubated with different concentration of **FL-CyN**, **FL**, **CyN**, Fluorescein and **ICG** at 37 °C for 8 h.

with dual excitation peaks can easily distinct the FRET-sensitized emission and direct-excited acceptor emission when using 460 nm as excitation wavelength. The two-photon property of the donor also help the chemosensor totally get rid of the direct-excited acceptor emission for the FRET sensing method and achieve the more accurate FRET results. Through time-resolved technology, the long-lifetime luminescence of the donor **FL** can efficiently diminish the autofluorescence interference from biological matrix.

We demonstrated that the special FRET system can work for sensing hypochlorite in the zebrafish. This is a typical of acceptor depletion FRET, which is considered as a kind of simple but potentially accurate FRET measurement. There is another non-destructive quantification FRET called acceptor-sensitized emission FRET which has more difficulty in achieving accurate FRET measurement [11]. We believe it is possible to develop a more accurate FRET sensing platform based on these special donor-acceptor pairs shown in this work.

Acknowledgements

This work was supported financially by the NNSF of China (21421005, 21576038), the Fundamental Research Funds for the Central Universities of China (DUT16TD21), and Science Program of Dalian City (2014J11JH133, 2015J12JH207).

Appendix A. Supplementary data

Supplementary data associated with this article can be found, in the online version, at https://doi.org/10.1016/j.snb.2018.01.240.

References

[1] E.M. Obeng, et al., FRET spectroscopy-towards effective biomolecular probing, Anal. Methods 8 (27) (2016) 5323–5337.
[2] B. Hochreiter, A. Garcia, J. Schmid, Fluorescent proteins as genetically encoded FRET biosensors in life sciences, Sensors 15 (10) (2015) 26281–26314.
[3] E.A. Jares-Erijman, T.M. Jovin, Imaging molecular interactions in living cells by FRET microscopy, Curr. Opin. Chem. Biol. 10 (2006) 409–416.
[4] M.S. Tremblay, M. Halim, D. Sames, Cocktails of Tb3+ and Eu3+ complexes: a general platform for the design of ratiometric optical probes, J. Am. Chem. Soc. 129 (24) (2007) 7570–7577.
[5] S. Padilla-Parra, M. Tramier, FRET microscopy in the living cell: different approaches, strengths and weaknesses, Bioessays (2012) 369–376.
[6] J.C. Waters, Accuracy and precision in quantitative fluorescence microscopy, J. Cell Biol. 185 (7) (2009) 1135–1148.
[7] M. Du, et al., Wide-field microscopic FRET imaging using simultaneous spectral unmixing of excitation and emission spectra, Opt. Express 24 (14) (2016) 16037.
[8] G. Clemens, et al., Vibrational spectroscopic methods for cytology and cellular research, Analyst 139 (18) (2014) 4411–4444.
[9] M.A. Rizzo, et al., Optimization of pairings and detection conditions for measurement of FRET between cyan and yellow fluorescent proteins, Microsc. Microanal. 12 (03) (2006) 238–254.
[10] H. Li, H. Yu, T. Chen, Partial acceptor photobleaching-based quantitative FRET method completely overcoming emission spectral crosstalks, Microsc. Microanal. 18 (05) (2012) 1021–1029.
[11] Y. Gu, et al., Quantitative fluorescence resonance energy transfer (FRET) measurement with acceptor photobleaching and spectral unmixing, J. Microsc. 215 (Pt 2) (2004) 162–173.
[12] G. Chen, et al., FRET spectral unmixing: a ratiometric fluorescent nanoprobe forhypochloritew, Chem. Comm. (Camb.) 48 (2012) 2949–2951.
[13] M. Cardoso Dos Santos, N. Hildebrandt, Recent developments in lanthanide-to-quantum dot FRET using time-gated fluorescence detection and photon upconversion, TrAC Trends Anal. Chem. 84 (2016) 60–71.
[14] S. Padilla-Parra, et al., Non fitting based FRET-FLIM analysis approaches applied to quantify protein–protein interactions in live cells, Biophys. Rev. 3 (2) (2011) 63–70.
[15] W. Zheng, et al., Time-resolved luminescent biosensing based on inorganic lanthanide-doped nanoprobes, Chem. Comm. 51 (2015) 4129–4143.
[16] D. Tu, et al., Time-resolved FRET biosensor based on amine-functionalized lanthanide-foped NaYF4 nanocrystals, Angew. Chem. Int. Ed. 50 (28) (2011) 6306–6310.
[17] X. Peng, et al., Heptamethine cyanine dyes with a large stokes shift and strong fluorescence: a paradigm for excited-state intramolecular charge transfer, J. Am. Chem. Soc. 127 (12) (2005) 4170–4171.
[18] G. Cheng, et al., A near-infrared fluorescent probe for selective detection of HClO based on Se-sensitized aggregation of heptamethine cyanine dye, Chem. Commun. 50 (8) (2014) 1018–1020.
[19] Z. Lou, Ratiometric fluorescence imaging of cellular hypochlorous acid based on heptamethine cyanine dyes, Analyst 138 (21) (2013) 6291.
[20] D. Oushiki, et al., Development and application of a near-infrared fluorescence probe for oxidative stress based on differential reactivity of linked cyanine dyes, J. Am. Chem. Soc. 132 (8) (2010) 2795–2801.
[21] X. Xiong, et al., Thermally activated delayed fluorescence of fluorescein derivative for time-resolved and confocal fluorescence imaging, J. Am. Chem. Soc. 136 (27) (2014) 9590–9597.
[22] H.E. Rajapakse, et al., Time-resolved luminescence resonance energy transfer imaging of protein–protein interactions in living cells, Proc. Natl. Acad. Sci. 107 (31) (2010) 13582–13587.
[23] H. Saneyoshi, Y. Ito, H. Abe, Long-lived luminogenic probe for detection of RNA in a crude solution of living bacterial cells, J. Am. Chem. Soc. 135 (37) (2013) 13632–13635.
[24] S. Padilla-Parra, et al., Non fitting based FRET-FLIM analysis approaches applied to quantify protein–protein interactions in live cells, Biophys. Rev. 3 (2) (2011) 63–70.
[25] X. Chen, et al., Recent progress in the development of fluorescent: luminescent and colorimetric probes for detection of reactive oxygen and nitrogen species, Chem. Soc. Rev. 45 (10) (2016) 2976–3016.
[26] H. Xiao, et al., A fast-responsive mitochondria-targeted fluorescent probe detecting endogenous hypochlorite in living RAW 264.7 cells and nude mouse, Chem. Commun. (Camb.) 51 (8) (2015) 1442–1445.
[27] L. Wu, et al., Photostable ratiometric pdot probe for in vitro and in vivo imaging of hypochlorous acid, J. Am. Chem. Soc. 139 (20) (2017) 6911–6918.